

g Factor of Lithiumlike Silicon: New Challenge to Bound-State QEDD. A. Glazov,¹ F. Köhler-Langes,² A. V. Volotka,^{1,3,4} K. Blaum,² F. Heiße,^{2,4} G. Plunien,⁵ W. Quint,⁴ S. Rau,² V. M. Shabaev,¹ S. Sturm,² and G. Werth⁶¹*Department of Physics, St. Petersburg State University, Universitetskaya 7/9, 199034 St. Petersburg, Russia*²*Max-Planck-Institut für Kernphysik, Saupfercheckweg 1, D-69117 Heidelberg, Germany*³*Helmholtz-Institut Jena, Fröbelstieg 3, D-07743 Jena, Germany*⁴*GSI Helmholtzzentrum für Schwerionenforschung GmbH, Planckstraße 1, D-64291 Darmstadt, Germany*⁵*Institut für Theoretische Physik, Technische Universität Dresden, Mommsenstraße 13, D-01062 Dresden, Germany*⁶*Institut für Physik, Johannes Gutenberg-Universität, D-55099 Mainz, Germany*

(Received 27 March 2019; revised manuscript received 31 August 2019; published 25 October 2019)

The recently established agreement between experiment and theory for the g factors of lithiumlike silicon and calcium ions manifests the most stringent test of the many-electron bound-state quantum electrodynamics (QED) effects in the presence of a magnetic field. In this Letter, we present a significant simultaneous improvement of both theoretical $g_{\text{th}} = 2.000\,889\,894\,4(34)$ and experimental $g_{\text{exp}} = 2.000\,889\,888\,45(14)$ values of the g factor of lithiumlike silicon $^{28}\text{Si}^{11+}$. The theoretical precision now is limited by the many-electron two-loop contributions of the bound-state QED. The experimental value is accurate enough to test these contributions on a few percent level.

DOI: [10.1103/PhysRevLett.123.173001](https://doi.org/10.1103/PhysRevLett.123.173001)

Introduction.—The magnetic moment of elementary particles and simple systems is a perfect tool for testing fundamental theories. High-precision g -factor measurements in highly charged ions [1–8] in combination with elaborate theoretical investigations (see, e.g., Refs. [9,10] for reviews) have provided the most stringent test of bound-state QED in the presence of a magnetic field to date. It keeps up with the accurate QED tests with binding energies [11,12] and hyperfine splittings [13–15] in the strong electromagnetic field of heavy nuclei; see also Refs. [16–18] for reviews. Meanwhile, unprecedented experimental and theoretical precision of the g factor of middle- Z ions provides the probes of the nontrivial bound-state QED effects which are only accessible otherwise in heavy ions. Furthermore, bound-electron g -factor studies resulted in the most accurate value of the electron mass [19–22]. Recent measurements with two highly charged lithiumlike calcium isotopes [6] have demonstrated the possibility to access the relativistic nuclear recoil effect [23–25]. This effect represents bound-state QED beyond the Furry picture in the strong coupling regime, i.e., beyond the external-field approximation where the nucleus is treated merely as a source of the classical electromagnetic field. While hydrogenlike ions, due to their simplicity, allow for the most accurate theoretical predictions, nuclear effects set the ultimate limits of the theoretical accuracy regardless of the progress in QED calculations. However, in combination with measurements on lithiumlike and boron-like ions, these limits can be overcome [26,27]. Here, specific differences of the g -factor values of different charge states with the same nucleus exhibit orders-of-magnitude smaller

theoretical uncertainties than the individual g factors [26–30]. Based on this, an independent determination of the fine structure constant from heavy hydrogen- and boron-like ions [27] and from light hydrogenlike and lithiumlike ions [29] has been proposed. Following the experiments with hydrogenlike ions [1–4], the g factor of lithiumlike silicon has been measured at Mainz University with a relative uncertainty of 1.1×10^{-9} [5]. Shortly after, the g factors of two lithiumlike calcium isotopes have been measured with 2 times smaller uncertainty [6]. The corresponding efforts devoted to the evaluation of the many-electron contributions to the g factor of three-electron ions have led to a relative theoretical uncertainty of 3×10^{-9} for silicon [31] and 6×10^{-9} for calcium [32].

In this Letter, we present simultaneous experimental (by a factor of 15) and theoretical (by a factor of 2) improvements of the g factor of lithiumlike silicon. In view of the determination of the fine structure constant [29] this represents an important step towards this long-term goal. The experimental progress is mainly due to the phase-sensitive pulse and amplify (PnA) method used for determination of the ion's cyclotron frequency. The theoretical improvement is based on the reevaluation of the interelectronic-interaction effects within the recursive formulation of the perturbation theory. As a result, the theoretical uncertainty is now dominated by the contributions of the next-order many-electron QED diagrams. In order to achieve further progress, these contributions need to be evaluated rigorously (to all orders in αZ), while the remaining theoretical background is sufficiently developed to match the present experimental accuracy.

Experiment.—The Zeeman splitting of the electron energy levels in a homogeneous magnetic field B : $\Delta E = h\nu_L = hgeB/(4\pi m_e)$ gives experimental access to the bound-electron g factor. Here, h denotes the Planck constant, ν_L the Larmor frequency, e the electric charge of the electron, and m_e its mass. By measuring the cyclotron frequency of the highly charged ion $\nu_c = q_{\text{ion}}B/(2\pi m_{\text{ion}})$, where q_{ion} is the electric charge and m_{ion} is the mass of the ion, the magnetic field can be determined and the g factor is then given by the ratios of frequencies ($\Gamma \equiv \nu_L/\nu_c$), masses (m_e/m_{ion}), and charges (q_{ion}/e):

$$g = 2\Gamma \frac{m_e}{m_{\text{ion}}} \frac{q_{\text{ion}}}{e}. \quad (1)$$

In the case of lithiumlike silicon, the mass of the ion $m(^{28}\text{Si}^{11+}) = 27.970\,894\,575\,55(75)$ u [20,33,34] and the mass of the electron $m_e = 0.000\,548\,579\,909\,070(16)$ u [19,20,35] contribute to the relative systematic uncertainty of the experimentally determined g factor on a level of $\delta g/g|_{m_{\text{ion}}, m_e} = 4 \times 10^{-11}$, whereas the previously measured frequency ratio Γ entails a relative uncertainty of $\delta g/g|_{\Gamma} = 1 \times 10^{-9}$ [5]. In the following, a 15-fold improved value of Γ is presented.

For the determination of the Larmor-to-cyclotron frequency ratio Γ , the experimental apparatus for bound-electron g factors of highly charged ions, located in Mainz, has been used [35]. Here, a single $^{28}\text{Si}^{11+}$ ion is studied inside a stack of cylindrical Penning traps of 3.5 mm radius. This stack is placed into a hermetically sealed vacuum vessel permeated by a homogeneous 3.8 T magnetic field and cooled to the temperature of liquid helium. The cryogenic temperature enables reaching an extraordinarily good vacuum in excess of 10^{-17} mbar, such that the highly charged ions can be stored for periods in excess of several weeks. Generally, most electrodes in the stack are kept at ground potential. By applying a voltage of about -7.2 V to the so-called ring electrode of the “precision trap” (PT), the ion is confined in the direction parallel to the magnetic field lines. Additionally, a set of correction electrodes allows improving the harmonicity of the resulting electrostatic potential significantly. In the combined electrostatic and magnetic field the ion undergoes a motion that can be decomposed into the three independent harmonic oscillations, the axial motion along the magnetic field lines in the axial direction with the frequency $\nu_z = 631$ kHz and the two modes in the radial direction, the (modified) cyclotron mode at $\nu_+ = 22.7$ MHz and the magnetron motion with $\nu_- = 8.8$ kHz. The axial motion can be detected via the image currents that the ion induces onto the trap electrodes. A superconducting resonant “tank” circuit with high effective resistance at resonance converts the induced femto-ampere current into measurable nanovoltages and, moreover, cools the ion’s axial motion to 4K. In thermal equilibrium the ion effectively shorts the tank circuit at its

axial frequency and consequently can be seen as a minimum (“dip”) in the thermal noise spectrum. The radial motions do not couple directly to the tank circuit, but can be coupled to the axial motion via suitable radiofrequency excitations at the respective sum or difference frequencies [36,37]. For the most important modified cyclotron mode we use the phase-sensitive PnA method, which allows a Ramsey-type detection at low motional amplitudes and correspondingly small systematic shifts [38]. With all eigenfrequencies measured, the free cyclotron frequency can be reconstructed even in the presence of field imperfections using the Brown-Gabrielse invariance relation $\nu_c = \sqrt{\nu_+^2 + \nu_z^2 + \nu_-^2}$ [39]. The second ingredient for the sought-after ratio Γ , the Larmor precession frequency $\nu_L = 105$ GHz, is determined by performing millimeter-wave spectroscopy on the transition between the Zeeman sublevels. To this end, we detect the magnetic sublevel, or spin state, using the continuous Stern-Gerlach effect (CSGE) [40] in a second, dedicated so-called “analysis trap” (AT). Here, a ferromagnetic ring electrode creates a strong magnetic inhomogeneity of the form $B_z = B_0 + B_2 z^2 + \dots$ with $B_2 = 10.5$ kT/m². In this field, the ion experiences an additional axial force which depends on the magnetic moment projection and consequently slightly alters the axial frequency. In the case of the $^{28}\text{Si}^{11+}$ ion discussed here, a spin-flip causes a clearly detectable axial frequency jump of about 260 mHz. To avoid adverse effects of the magnetic bottle on the precision of the measurement, we perform the precision spectroscopy of Γ in the spatially separated PT. Here, the cyclotron frequency is measured, which takes about 5 sec, and simultaneously a millimeter wave at a random probe frequency ν_{mw} is injected. Afterwards, we transport the ion into the AT, where we detect the spin state via the CSGE. The result is compared to the one of the previous cycle to determine whether the millimeter wave in the PT has effectively flipped the spin state. This way, we can map the spin-flip probability as a function of the ratio of the measured cyclotron frequency and the chosen millimeter-wave frequency $\Gamma^* = \nu_{\text{mw}}/\nu_c$ and apply a maximum likelihood fit to the data set with a Gaussian distribution. From this we extract the center Γ_{stat} , which we subsequently correct for systematic shifts. Further details on the measurement cycle can be found, e.g., in Ref. [35]. Compared to the previous campaign [5], we have increased the precision per cycle by about an order of magnitude by using the phase-sensitive PnA method rather than the noise dips for the modified frequency detection. Furthermore, the time required in the AT for spin-flip detection has been reduced significantly by increasing the available millimeter-wave power and by improving the centering of the ion in the AT. If the ion is shifted from the center of the bottle, e.g., by stray electric fields arising from imperfections on the electrode surfaces or by geometric misalignment of the trap electrodes, the Larmor precession becomes strongly modulated by the

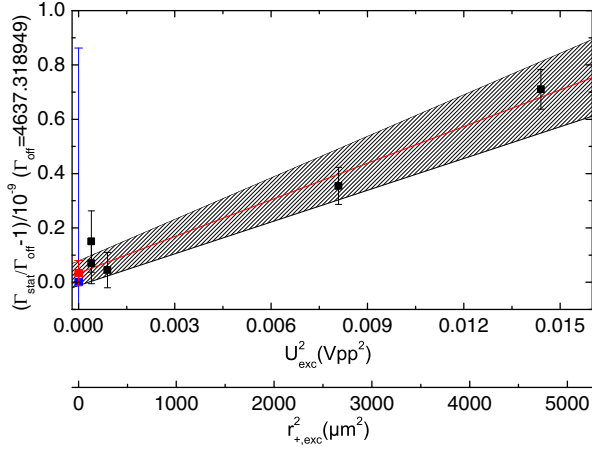


FIG. 1. Measured frequency ratios Γ_{stat} at different modified cyclotron excitation energies during the PnA cycle minus some offset parameter Γ_{off} . At a fixed pulse length, the excited modified cyclotron radius $r_{+,exc}$ scales linearly with the amplitude U_{exc} of the first PnA pulse measured in voltage peak to peak (Vpp). Since the dominant relativistic shift depends quadratically on the radius, data are plotted versus $r_{+,exc}^2$. The red line indicates a linear fit extrapolating to zero excitation energy. The extrapolated value (red dot with error bar) is in excellent agreement with the former measurement (blue dot with error bar) [5]. The gray hatched area indicates the uncertainty of the linear fit.

axial motion, as can be seen from the expansion of the magnetic bottle field around an offset δz : $B(t) = B_0 + 2B_z \delta z z(t) + \dots$. Consequently, a series of axial sidebands appears and significantly reduces the effectively available millimeter-wave power. This effect can be counteracted by applying suitable correction voltages which shift the ion back into the (axial) center of the bottle.

In 1.5 months, 1674 measurement cycles (263 cycles with and 1411 cycles without a spin-flip in the PT) have been recorded at four different modified cyclotron excitation radii $r_{+,exc} = 11, 17, 52, 69 \mu\text{m}$, see Fig. 1. Here, the slope is mainly given by the relativistic shift of the modified cyclotron energy. The linearly extrapolated frequency ratio at zero excitation energy $\Gamma_{\text{stat}}(r_{+,exc} = 0) = 4637.31894916(21)$ has to be corrected for systematic shifts, see Table I, which are also discussed in Ref. [35]:

$$\Gamma_{\text{final}}(^{28}\text{Si}^{11+}) = 4637.31894610(27). \quad (2)$$

The additional electric field, which is generated by the induced image charges on the trap surfaces, causes small shifts in the two radial frequencies [4]. This so-called image charge shift is the dominant systematic effect [41]. In combination with the masses given above we determine an improved value of the bound-electron g factor of lithium-like silicon:

$$g_{\text{exp}}(^{28}\text{Si}^{11+}) = 2.000889888450(92)(68)(53)(58). \quad (3)$$

TABLE I. Relative systematic shifts of the frequency ratio Γ and their uncertainties, defined as $(\Gamma_{\text{final}} - \Gamma_{\text{stat}})/\Gamma_{\text{off}}$.

Effect	Rel. shift ($\times 10^{12}$)	Rel. uncert. ($\times 10^{12}$)
Image charge	-659	33
Line shape model	0	7
Residual electrostatic anharmonicity	$\ll 1$	2
Magnetron frequency uncertainty	0	2
Image current	-1	1
Residual magnetostatic inhomogeneity	0.5	0.4
Residual special relativity	-0.2	0.3
Total	-660	34

Here, the statistical and systematic uncertainty of Γ as well as the uncertainties due to the mass of $^{28}\text{Si}^{11+}$ and the mass of the electron are given in the four brackets separately. Our new value is in excellent agreement with the former measurement and exceeds its precision by a factor of 15. With a relative uncertainty of 7.0×10^{-11} , this new value also surpasses by a factor of 6 the precision of the currently most accurate lithiumlike g factor [$\delta g_{\text{exp}}(^{48}\text{Ca}^{17+})/g = 4.1 \times 10^{-10}$ [6]] which is limited by the uncertainty of the calcium ion mass.

Theory.—While for one-electron systems the theoretical consideration of the g factor comes down to the QED and nuclear effects, for lithiumlike ions the electron-electron interaction effects come into play. In contrast to other atomic properties, such as binding energies, for the g factor these effects are purely relativistic; i.e., they vanish in the nonrelativistic limit. Moreover, the contribution of the negative-energy states is not suppressed as compared to the positive-energy states and is equally important. These features make the g -factor evaluation in many-electron systems more involved than, e.g., the evaluation of the binding energies. Various calculation methods have been employed over the years, which resulted in today's accuracy on the level of 10^{-9} . In general, there are three expansion parameters that can be used in the theoretical description of highly charged ions: α , αZ , and $1/Z$, where α is the fine structure constant and Z is the nuclear charge number. Different theoretical approaches rely on the expansions in αZ , $1/Z$, or both. The rigorous QED approach accounts for all orders in αZ , while only few leading orders in α and $1/Z$ are accessible to date. In particular, the diagrams of the one- and two-photon exchange ($\sim 1/Z$ and $\sim 1/Z^2$) and the two-electron self-energy and vacuum-polarization diagrams ($\sim \alpha/Z$) have been evaluated to all orders in αZ [5,32,42,43]. In turn, the so-called NRQED (nonrelativistic quantum electrodynamics) approach provides access to all orders in $1/Z$ (based on the Schrödinger equation); however, it is restricted to

the leading orders in αZ (see, e.g., Refs. [31,44]). The interelectronic-interaction operator incorporating the leading relativistic corrections is known as the Coulomb-Breit operator. For this reason, the term “Breit approximation” is widely used for the results obtained with this operator and more generally for the results, which reproduce correctly the contributions to the g factor of the order $(\alpha Z)^2$. The higher-order remainder (starting from $(\alpha Z)^4$) can be termed as a “nontrivial QED contribution.” However, this separation depends on the exact formulation of the approach used to obtain the Breit approximation.

The interelectronic-interaction effects determine the accuracy of the recently published theoretical g -factor values [31,32] in the middle- Z region. For this reason, below we consider these effects in some detail. According to the previous works, we separate the many-electron contributions into the pure interelectronic-interaction correction, the screening of the QED effects, and the corresponding correction to the nuclear recoil effect. The effect of the finite nuclear size can be taken into account for each of these contributions by using the Coulomb potential of the finite nucleus.

First, we consider the interelectronic-interaction correction to the g factor of lithiumlike ions within the Breit approximation. Accurate calculations to all orders in $1/Z$ have been performed by Yan [45,46] based on the effective two-component Hamiltonian derived by Hegstrom [47]. Recently, Yerokhin and co-authors have performed similar calculations with much better accuracy [31]. In this work, we present an independent calculation within the recursive formulation of the perturbation theory [48]. This method proved to be efficient for calculations of the higher-order interelectronic-interaction contributions to the binding energies in few-electron ions [48–50]. Presently, the method is further developed to the g -factor calculations. This implies, in particular, proper accounting for the contribution of the negative-energy continuum which is a tricky problem, often solved incorrectly within the established methods, see, e.g., discussion in Refs. [51,52]. Application to the nuclear-recoil effect on the g factor has been demonstrated already in Refs. [23,25]. The key advantage of this method is that it provides direct access to the individual terms of the $1/Z$ expansion. Consequently, no fitting procedure is needed to identify the part of the order $1/Z^3$ and higher, which is to be combined with the QED values for the $1/Z$ and $1/Z^2$ terms. The convergence of the $1/Z$ expansion can be improved significantly by using the effective screening potential in the Dirac equation, which defines the zeroth-order wave functions. We consider three different screening potentials—core-Hartree, Kohn-Sham, and local Dirac-Fock [49,53–56]. As a result, we find the Breit-approximation part of the interelectronic interaction with an uncertainty on the level of 1×10^{-9} . It has to be complemented by the nontrivial QED contribution (higher orders in αZ) evaluated with the same screening potential.

Evaluation of the interelectronic interaction to all orders in αZ within the framework of bound-state QED can be done only order by order in $1/Z$. The first-order correction (one-photon exchange) is relatively simple, it has been calculated, e.g., in Ref. [26] for a wide range of Z . The two-photon-exchange correction is significantly more involved, including the derivation of the complete set of formulas and development of the numerical procedure. The first evaluation for lithiumlike silicon with the Coulomb potential in Ref. [5] was extended to several other lithiumlike ions and to various screening potentials in Ref. [32]. In this paper, we reevaluate the one- and two-photon-exchange contributions for silicon with the potentials listed above to match the Breit-approximation values. The total interelectronic-interaction contribution to the g factor of lithiumlike silicon is $314.8118(12)(24) \times 10^{-6}$. The first error bar here is the numerical uncertainty of the calculations. The second one is due to the unknown nontrivial QED contribution of the three-photon-exchange diagrams. It can be estimated based on different ratios of the presently known contributions. As an approximate average of these estimations, we use the expression $2(\alpha Z)^2 \Delta g^{(3)}$, where $\Delta g^{(3)}$ is the $1/Z^3$ contribution evaluated in the Breit approximation. This estimation is more conservative than the one used in Ref. [31].

The interplay between the interelectronic interaction and QED effects leads to the two-electron or “screened” QED correction. In analogy to the “pure” interelectronic-interaction contribution considered above, one can also consider the Breit approximation here. To this end, one can use the set of two-component effective QED operators [47]. For s states these operators yield the correct result up to the order $(\alpha Z)^2$ for arbitrary order in α and $1/Z$. In Refs. [31,45,46] these operators were used to evaluate the screened QED correction by averaging with the many-electron wave functions obtained from the many-electron Schrödinger equation. In Ref. [51] the four-component counterparts of these operators were used to calculate the $1/Z$ contribution. In this work, we incorporate these operators in the recursive perturbation theory in order to find the contributions of arbitrary order in $1/Z$. In order to obtain the sought-for contributions we develop the multi-recursive scheme of the perturbation theory with respect to the following operators: the effective four-component QED operators (first order), the magnetic-field interaction (first order), and the interelectronic interaction (arbitrary order). In addition, we employ the effective screening potential (see above), which accelerates the convergence of the perturbation series in $1/Z$.

Screened QED correction of the first orders in α and in $1/Z$ corresponds to the set of two-electron self-energy and vacuum-polarization diagrams, which have been evaluated to all orders in αZ in Refs. [32,42,43]. The numerical uncertainty of these calculations gets larger for smaller nuclear charge due to the large cancellations of individual terms and the poor partial-wave convergence. In this work,

TABLE II. Individual contributions to the ground-state g factor of lithiumlike silicon and comparison with the experimental result and with the previously reported theoretical and experimental values. The experimental result of Wagner *et al.* [5] is updated for the new values of the electron mass and the mass of $^{28}\text{Si}^{11+}$.

Dirac value (point nucleus)	1.998 254 750 7
Finite nuclear size	0.000 000 002 6
QED, $\sim\alpha$	0.002 324 043 9
QED, $\sim\alpha^2+$	-0.000 003 516 6 (3)
Interelectronic interaction	0.000 314 811 8 (27)
Screened QED	-0.000 000 241 5 (21)
Nuclear recoil	0.000 000 043 6
Total theory, this work	2.000 889 894 4 (34)
Total theory, Yerokhin <i>et al.</i> [31]	2.000 889 892 (6)
Total theory, Volotka <i>et al.</i> [32]	2.000 889 892 (8)
Experiment, this work	2.000 889 888 450 (139)
Experiment, Wagner <i>et al.</i> [5]	2.000 889 888 4 (19) ^a

^aUpdated for the involved mass values (see text).

in order to get the most of both the rigorous approach and the effective operators, we have performed the calculations within both methods for a set of Z in the range 20–50. Then the difference between these values has been extrapolated to $Z = 14$ by fitting to the polynomials in $1/Z$ and αZ . As a result, we find $-0.2415(14)(16) \times 10^{-6}$ for the screened QED correction to the g factor of lithiumlike silicon. The first given uncertainty is numerical and the second one is due to the unknown nontrivial QED contribution of the second and higher orders in $1/Z$. It is estimated using the ratio of the nontrivial QED contribution and the Breit-approximation part of the $1/Z$ contribution, in full agreement with Ref. [31].

The theoretical results for the g factor of lithiumlike silicon are summarized in Table II. The finite nuclear size effect is calculated numerically, the uncertainties due to the nuclear radius and model are negligible at present. The interelectronic-interaction and the screened QED contributions are evaluated in the present work as described above. The one-loop one-electron QED correction is taken from Refs. [51,57,58]. The QED correction of the second and higher orders in α obtained within the framework of αZ expansion is taken from Refs. [22,31,59,60]. For the nuclear recoil effect we use the most recent results from Refs. [23,25], which include the higher-order terms in αZ and the interelectronic-interaction contributions. The total theoretical value of the g factor is

$$g_{\text{th}}(^{28}\text{Si}^{11+}) = 2.000\,889\,894\,4(34). \quad (4)$$

The error bar is largely determined by the estimation of the presently unknown contributions of the two-loop many-electron diagrams: three-photon exchange and two-photon exchange with additional self-energy loop. The difference

between g_{th} and g_{exp} is 1.7 times larger than this uncertainty, which strongly stimulates further theoretical investigations.

Conclusion.—In summary, we have presented a 15-fold improvement of the experimental value and a twofold improvement of the theoretical value of the g factor of $^{28}\text{Si}^{11+}$. The experimental and theoretical relative uncertainties amount to 7.0×10^{-11} and 1.7×10^{-9} , respectively. The latter is mostly determined by the unknown many-electron two-loop QED contributions. The obtained values are 1.7σ apart, which may indicate that these contributions exceed our present estimations. Further laborious developments of the theoretical methods are required to resolve this discrepancy. At the same time, the obtained experimental value has a potential to validate the nontrivial parts of the many-electron two-loop QED contributions on a few percent level as soon as they are calculated.

This work was supported by RFBR (Grants No. 16-02-00334 and No. 19-02-00974), by DFG (Grant No. VO 1707/1-3), by SPbSU-DFG (Grants No. 11.65.41.2017 and No. STO 346/5-1), by SPbSU (COLLAB 2019: 37715081), by the Max Planck Society, by the International Max Planck Research School for Quantum Dynamics in Physics, Chemistry and Biology (IMPRS-QD), and by the International Max Planck Research School for Precision Tests of Fundamental Symmetries in Particle Physics, Nuclear Physics, Atomic Physics and Astroparticle Physics (IMPRS-PTFS) at the University of Heidelberg. This work is part of and supported by the German Research Foundation (DFG) Collaborative Research Centre ‘‘SFB 1225 (ISOQUANT)’’.

- [1] H. Häffner, T. Beier, N. Hermanspahn, H.-J. Kluge, W. Quint, S. Stahl, J. Verdú, and G. Werth, *Phys. Rev. Lett.* **85**, 5308 (2000).
- [2] J. Verdú, S. Djekić, S. Stahl, T. Valenzuela, M. Vogel, G. Werth, T. Beier, H.-J. Kluge, and W. Quint, *Phys. Rev. Lett.* **92**, 093002 (2004).
- [3] S. Sturm, A. Wagner, B. Schabinger, J. Zatorski, Z. Harman, W. Quint, G. Werth, C. H. Keitel, and K. Blaum, *Phys. Rev. Lett.* **107**, 023002 (2011).
- [4] S. Sturm, A. Wagner, M. Kretschmar, W. Quint, G. Werth, and K. Blaum, *Phys. Rev. A* **87**, 030501(R) (2013).
- [5] A. Wagner, S. Sturm, F. Köhler, D. A. Glazov, A. V. Volotka, G. Plunien, W. Quint, G. Werth, V. M. Shabaev, and K. Blaum, *Phys. Rev. Lett.* **110**, 033003 (2013).
- [6] F. Köhler, K. Blaum, M. Block, S. Chenmarev, S. Eliseev, D. A. Glazov, M. Goncharov, J. Hou, A. Kracke, D. A. Nesterenko, Yu. N. Novikov, W. Quint, E. M. Ramirez, V. M. Shabaev, S. Sturm, A. V. Volotka, and G. Werth, *Nat. Commun.* **7**, 10246 (2016).
- [7] I. Arapoglou, A. Egl, M. Höcker, T. Sailer, B. Tu, A. Weigel, R. Wolf, H. Cakir, V. A. Yerokhin, N. S. Oreshkina, V. A. Agababaev, A. V. Volotka, D. V. Zinenko, D. A. Glazov, Z. Harman, C. H. Keitel, S. Sturm, and K. Blaum, *Phys. Rev. Lett.* **122**, 253001 (2019).

- [8] S. Sturm, M. Vogel, F. Köhler-Langes, W. Quint, K. Blaum, and G. Werth, *Atoms* **5**, 4 (2017).
- [9] V. M. Shabaev, D. A. Glazov, G. Plunien, and A. V. Volotka, *J. Phys. Chem. Ref. Data* **44**, 031205 (2015).
- [10] Z. Harman, B. Sikora, V. A. Yerokhin, H. Cakir, V. Debierre, N. Michel, N. S. Oreshkina, N. A. Belov, J. Zatorski, and C. H. Keitel, *J. Phys. Conf. Ser.* **1138**, 012002 (2018).
- [11] A. Gumberidze, Th. Stöhlker, D. Banaś, K. Beckert, P. Beller, H. F. Beyer, F. Bosch, S. Hagmann, C. Kozhuharov, D. Liesen, F. Nolden, X. Ma, P. H. Mokler, M. Steck, D. Sierpowski, and S. Tashenov, *Phys. Rev. Lett.* **94**, 223001 (2005).
- [12] P. Beiersdorfer, H. Chen, D. B. Thorn, and E. Träbert, *Phys. Rev. Lett.* **95**, 233003 (2005).
- [13] A. V. Volotka, D. A. Glazov, O. V. Andreev, V. M. Shabaev, I. I. Tupitsyn, and G. Plunien, *Phys. Rev. Lett.* **108**, 073001 (2012).
- [14] J. Ullmann *et al.*, *Nat. Commun.* **8**, 15484 (2017).
- [15] L. V. Skripnikov, S. Schmidt, J. Ullmann, C. Geppert, F. Kraus, B. Kresse, W. Nörtershäuser, A. F. Privalov, B. Scheibe, V. M. Shabaev, M. Vogel, and A. V. Volotka, *Phys. Rev. Lett.* **120**, 093001 (2018).
- [16] A. V. Volotka, D. A. Glazov, G. Plunien, and V. M. Shabaev, *Ann. Phys. (Berlin)* **525**, 636 (2013).
- [17] M. G. Kozlov, M. S. Safronova, J. R. C. López-Urrutia, and P. O. Schmidt, *Rev. Mod. Phys.* **90**, 045005 (2018).
- [18] V. M. Shabaev, A. I. Bondarev, D. A. Glazov, M. Y. Kaygorodov, Y. S. Kozhedub, I. A. Maltsev, A. V. Malyshev, R. V. Popov, I. I. Tupitsyn, and N. A. Zubova, *Hyperfine Interact.* **239**, 60 (2018).
- [19] S. Sturm, F. Köhler, J. Zatorski, A. Wagner, Z. Harman, G. Werth, W. Quint, C. H. Keitel, and K. Blaum, *Nature (London)* **506**, 467 (2014).
- [20] P. J. Mohr, D. B. Newell, and B. N. Taylor, *Rev. Mod. Phys.* **88**, 035009 (2016).
- [21] J. Zatorski, B. Sikora, S. G. Karshenboim, S. Sturm, F. Köhler-Langes, K. Blaum, C. H. Keitel, and Z. Harman, *Phys. Rev. A* **96**, 012502 (2017).
- [22] A. Czarniecki, M. Dowling, J. Piclum, and R. Szafron, *Phys. Rev. Lett.* **120**, 043203 (2018).
- [23] V. M. Shabaev, D. A. Glazov, A. V. Malyshev, and I. I. Tupitsyn, *Phys. Rev. Lett.* **119**, 263001 (2017).
- [24] A. V. Malyshev, V. M. Shabaev, D. A. Glazov, and I. I. Tupitsyn, *Pis'ma Zh. Eksp. Teor. Fiz.* **106**, 731 (2017) [*JETP Lett.* **106**, 765 (2017)].
- [25] V. M. Shabaev, D. A. Glazov, A. V. Malyshev, and I. I. Tupitsyn, *Phys. Rev. A* **98**, 032512 (2018).
- [26] V. M. Shabaev, D. A. Glazov, M. B. Shabaeva, V. A. Yerokhin, G. Plunien, and G. Soff, *Phys. Rev. A* **65**, 062104 (2002).
- [27] V. M. Shabaev, D. A. Glazov, N. S. Oreshkina, A. V. Volotka, G. Plunien, H.-J. Kluge, and W. Quint, *Phys. Rev. Lett.* **96**, 253002 (2006).
- [28] A. V. Volotka and G. Plunien, *Phys. Rev. Lett.* **113**, 023002 (2014).
- [29] V. A. Yerokhin, E. Berseneva, Z. Harman, I. I. Tupitsyn, and C. H. Keitel, *Phys. Rev. Lett.* **116**, 100801 (2016).
- [30] V. A. Yerokhin, E. Berseneva, Z. Harman, I. I. Tupitsyn, and C. H. Keitel, *Phys. Rev. A* **94**, 022502 (2016).
- [31] V. A. Yerokhin, K. Pachucki, M. Puchalski, Z. Harman, and C. H. Keitel, *Phys. Rev. A* **95**, 062511 (2017).
- [32] A. V. Volotka, D. A. Glazov, V. M. Shabaev, I. I. Tupitsyn, and G. Plunien, *Phys. Rev. Lett.* **112**, 253004 (2014).
- [33] M. Wang, G. Audi, F. G. Kondev, W. J. Huang, S. Naimi, and X. Xu, *Chin. Phys. C* **41**, 030003 (2017).
- [34] A. Kramida, Yu. Ralchenko, J. Reader, and the NIST ASD Team, <http://physics.nist.gov/asd> (2017).
- [35] F. Köhler, S. Sturm, A. Kracke, G. Werth, W. Quint, and K. Blaum, *J. Phys. B* **48**, 144032 (2015).
- [36] D. J. Wineland and H. G. Dehmelt, *Int. J. Mass Spectrom. Ion Phys.* **16**, 338 (1975).
- [37] E. A. Cornell, R. M. Weisskoff, K. R. Boyce, and D. E. Pritchard, *Phys. Rev. A* **41**, 312 (1990).
- [38] S. Sturm, A. Wagner, B. Schabinger, and K. Blaum, *Phys. Rev. Lett.* **107**, 143003 (2011).
- [39] L. S. Brown and G. Gabrielse, *Rev. Mod. Phys.* **58**, 233 (1986).
- [40] H. Dehmelt, *Proc. Natl. Acad. Sci. U.S.A.* **83**, 3074 (1986).
- [41] M. Schuh, F. Heiße, T. Eronen, J. Ketter, F. Köhler-Langes, S. Rau, T. Segal, W. Quint, S. Sturm, and K. Blaum, *Phys. Rev. A* **100**, 023411 (2019).
- [42] A. V. Volotka, D. A. Glazov, V. M. Shabaev, I. I. Tupitsyn, and G. Plunien, *Phys. Rev. Lett.* **103**, 033005 (2009).
- [43] D. A. Glazov, A. V. Volotka, V. M. Shabaev, I. I. Tupitsyn, and G. Plunien, *Phys. Rev. A* **81**, 062112 (2010).
- [44] A. Wienczek, M. Puchalski, and K. Pachucki, *Phys. Rev. A* **90**, 022508 (2014).
- [45] Z.-C. Yan, *Phys. Rev. Lett.* **86**, 5683 (2001).
- [46] Z.-C. Yan, *J. Phys. B* **35**, 1885 (2002).
- [47] R. A. Hegstrom, *Phys. Rev. A* **7**, 451 (1973); **11**, 421 (1975).
- [48] D. A. Glazov, A. V. Malyshev, A. V. Volotka, V. M. Shabaev, I. I. Tupitsyn, and G. Plunien, *Nucl. Instrum. Methods Phys. Res., Sect. B* **408**, 46 (2017).
- [49] A. V. Malyshev, D. A. Glazov, A. V. Volotka, I. I. Tupitsyn, V. M. Shabaev, G. Plunien, and Th. Stöhlker, *Phys. Rev. A* **96**, 022512 (2017).
- [50] A. V. Malyshev, Y. S. Kozhedub, D. A. Glazov, I. I. Tupitsyn, and V. M. Shabaev, *Phys. Rev. A* **99**, 010501(R) (2019).
- [51] D. A. Glazov, V. M. Shabaev, I. I. Tupitsyn, A. V. Volotka, V. A. Yerokhin, G. Plunien, and G. Soff, *Phys. Rev. A* **70**, 062104 (2004).
- [52] D. E. Maison, L. V. Skripnikov, and D. A. Glazov, *Phys. Rev. A* **99**, 042506 (2019).
- [53] W. Kohn and L. J. Sham, *Phys. Rev.* **140**, A1133 (1965).
- [54] J. Sapirstein and K. T. Cheng, *Phys. Rev. A* **66**, 042501 (2002).
- [55] V. M. Shabaev, I. I. Tupitsyn, K. Pachucki, G. Plunien, and V. A. Yerokhin, *Phys. Rev. A* **72**, 062105 (2005).
- [56] D. A. Glazov, A. V. Volotka, V. M. Shabaev, I. I. Tupitsyn, and G. Plunien, *Phys. Lett. A* **357**, 330 (2006).
- [57] R. N. Lee, A. I. Milstein, I. S. Terekhov, and S. G. Karshenboim, *Phys. Rev. A* **71**, 052501 (2005).
- [58] V. A. Yerokhin and Z. Harman, *Phys. Rev. A* **95**, 060501(R) (2017).
- [59] K. Pachucki, A. Czarniecki, U. D. Jentschura, and V. A. Yerokhin, *Phys. Rev. A* **72**, 022108 (2005).
- [60] A. Czarniecki and R. Szafron, *Phys. Rev. A* **94**, 060501(R) (2016).